

LOUIS MONCHICK

MOLECULAR SCATTERING EXPERIMENTS AT HIGH ALTITUDES

At very high altitudes, the overwhelming majority of molecules emanating from a spacecraft never return to it, and of those that do, most have never undergone more than one collision. The simple kinematics of this process allows the design of a molecular scattering experiment involving ambient oxygen atoms and beam molecules with a well-defined velocity originating from the spacecraft. Information on molecular forces can then be extracted from the return flux data, and a simple *ab initio* “back-of-the-envelope” approximation can be deduced for the return flux.

INTRODUCTION

The return flux of gases effusing from spacecraft is an important problem that has recently received much attention. Flux measurement experiments were included on the Midcourse Space Experiment (MSX) satellite, and some rather complicated rarefied gas dynamic codes¹⁻⁵ were developed to correlate the results. During discussions of the return fluxes, the question was raised as to whether the MSX results could be used to measure molecular forces. With the current MSX design, the answer “no” was quickly reached. However, a second question was raised, namely, could the MSX be redesigned so that molecular collision dynamics and molecular forces could be determined from the return flux measurements? This article discusses the results of these ruminations.

At shuttle altitudes, namely, 100 to 200 km, where the mean free path of molecules is of the same order of magnitude as the shuttle dimensions, the answer to the second question is almost certainly no because the molecular flux fields⁶ can be rather complicated, and the computer codes required to calculate them assume a correspondingly complex form. The complexities do not originate in unexpected intricacies in equations of flow or in molecular scattering processes, but rather in the complicated set of reflections from all the surfaces and the complex array of desorbing surfaces, leaks, and gas jet sources that the spacecraft presents to the environment. This complicated boundary and the associated uncertain boundary conditions, for instance, the fact that most molecular sources are not well defined or characterized, require codes that can account for all details of the flow fields near the spacecraft surface and all contingencies. The physics and chemistry of each fluid flow element are not complicated, but building enough detail and flexibility into the computer codes to account for a

complicated surface interacting with a complex environment makes the codes unduly intricate and oftentimes unwieldy.

At much higher altitudes, however, three characteristics of the environment simplify the problem considerably and make possible the experiment described here. These are (1) the reduction in the molecular flux fields according to s^{-2} , where s is the distance from the satellite, (2) the enormous mean free paths of molecules, resulting in extremely rare collisions of ambient and effusive molecules, and (3) satellite velocities much larger than gas kinetic speeds. In this article, I propose to show that these features can be used to design a scattering experiment in which force fields and cross sections can be deduced for molecules of moderate size and, as a side product, to derive a “back-of-the-envelope” approximation for the return flux of molecules originating from the spacecraft.

SPACECRAFT RETURN FLUXES

Consider a molecular beam emanating from a spacecraft surface confined within a narrow cone of solid angle $d\bar{\Omega} = \sin\theta d\bar{\theta} d\bar{\varphi}$, as shown schematically in Figure 1. This setup can be achieved with an aerodynamically designed beam source in wide use today. In a quasi-steady state, the total flux passing through all surfaces intersecting the cone must be conserved. This constraint implies that the flux density \mathbf{j} and the molecule density n_b at each point in the beam moving out from the satellite vary inversely with the square of the distance s from the spacecraft surface:

$$|\mathbf{j}(s)| \approx |\mathbf{j}(R)|(R/s)^2 \approx n_b(s) \mathbf{v}_b, \quad (1)$$



Figure 1. Schematic of a molecule (gray circle) leaving a satellite and encountering an ambient atmospheric molecule (black circle). The angle between the velocity vectors is $\bar{\theta}$.

$$n_b(s) \approx n_b(R) (R/s)^2, \quad (2)$$

where R is some length characterizing the general size of the spacecraft, and \mathbf{v}_b is the initial velocity of the beam molecules.

The distance s at which the detailed features of molecular flow will be lost need not be too much larger than R . This expectation is verified by calculations of molecular distributions using one of the new rarefied gas dynamics calculation techniques that has gained increasing acceptance, Direct Simulation Monte Carlo (DSMC)⁴⁻⁶ (see the boxed insert). The results of this method show that the density distribution of ambient molecules glancing off a satellite surface (see Fig. 2) at an altitude of 900 km and the density distribution of molecules desorbing from a small area on the topside of the satellite (see Fig. 3) both diminish as s^{-2} . Remarkable evidence of the absence of collisions is the shadow cast by the satellite in Figure 2. If appreciable numbers of collisions had occurred, that shadow would have been filled to some extent. More importantly, DSMC calculations can be used to design the satellite configuration so that the flow field of the ambient atmosphere encountered by the molecular beam will not be perturbed to any appreciable extent by the bow shock wave or the wake. As shown in Figure 4, this condition can be achieved by simply orienting the satellite to fly at an inclination of $\approx 9^\circ$ to ram. A slight vacuum is induced topside, but all boundary layers are confined to the bottom and sides.

DIRECT SIMULATION MONTE CARLO METHOD

Modern molecular dynamic studies other than Direct Simulation Monte Carlo (DSMC) generally follow the detailed motion of a small number of molecules, usually 1000 to 10,000, in a microscopic volume, usually less than 100 Å on a side. These studies are well suited to investigate reaction dynamics and continuum transport mechanisms, as well as all phenomena that depend only on molecular processes or do not involve macroscopic processes except as they affect the local environment parametrically. However, for flow problems in rarefied gases, macroscopic changes occur over distances comparable to the mean free path, that is, the average distance traveled by a gas molecule between successive collisions. Here, one must follow the molecular motion over macroscopic distances, which means following the motion of 10^{13} molecules at a pressure of one millionth of an atmosphere. Such tracking is obviously out of reach of even modern computers, so some approximate algorithm must be used. In the DSMC method, the gas molecules within a certain range of velocity and position are assigned to sets in the beginning of the calculation. (The name, Monte Carlo, refers to the fact that a random number generator is used to set the initial configuration of the simulated molecules and to determine the direction and magnitude of the velocity after every collision.) Thereafter, all the molecules in this set are assumed to move like the average molecule in the set. This assumption is referred to as replacing the original gas by a gas of "simulated molecules." Between collisions, a simulated molecule in a given set travels freely until it enters a volume occupied by another simulated molecule, at which point the collision probability is calculated from microscopic dynamics as if each of the molecules in the first set is colliding (with some suitably adjusted probability) with one of the molecules in the second set. Even if the number of simulated molecules N is very large—the calculations that generated Figures 2, 3, and 4 used 256,000 simulated molecules—and the rarefied gas dynamics is mimicked quite well, the magnitude of fluctuations, which by Einstein's fluctuation theorem is proportional to $N^{-1/2}$, is still observable. This difficulty, namely, the spuriously large density fluctuations observed at particular times, was overcome by averaging the flow field at suitable intervals. This averaging over time raised the effective number of simulated molecules to about 10^7 .

At very high altitudes, namely, higher than 900 km, the mean free path⁷ L will be much larger than R . It follows that from this viewpoint, not only will the spacecraft have lost its detailed features, but it will approximate both a point source of the initial flux and a point target for the return flux. Collisions with the ambient atmosphere always tend to knock molecules coming from the spacecraft downwind, gradually slowing them down to equilibrate with the ambient atmosphere. This situation implies that, until the next pass at least, only a few molecules (those that have traversed only a few improbable trajectories) will return to the spacecraft. The simplest case to consider is the set of molecules that return after a single collision, because only these will have a well-

Figure 2. The density of oxygen (atoms/ m^3) colliding with a satellite with two solar panels. The satellite is traveling to the left at 8 km/s, is at an altitude of about 900 km, and is inclined at an angle of about 9° . The viewing point is from the side. The density scale is shown to the right of the figure.

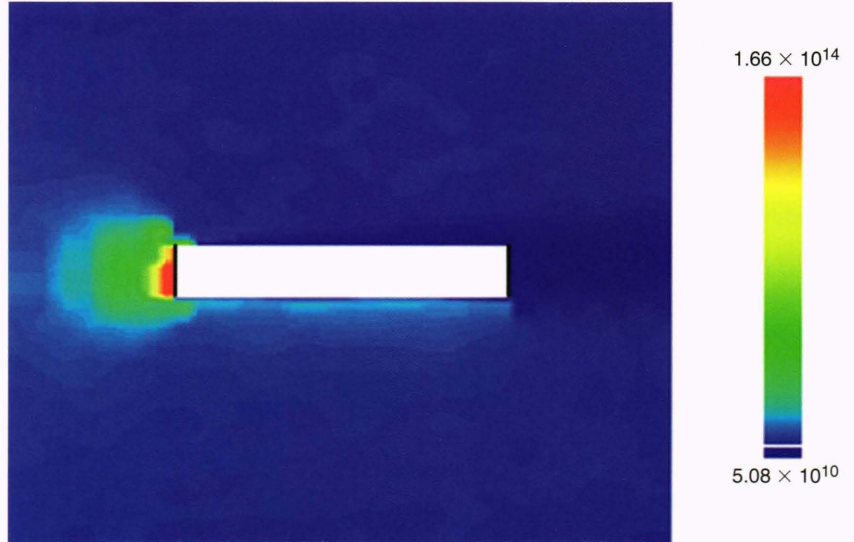
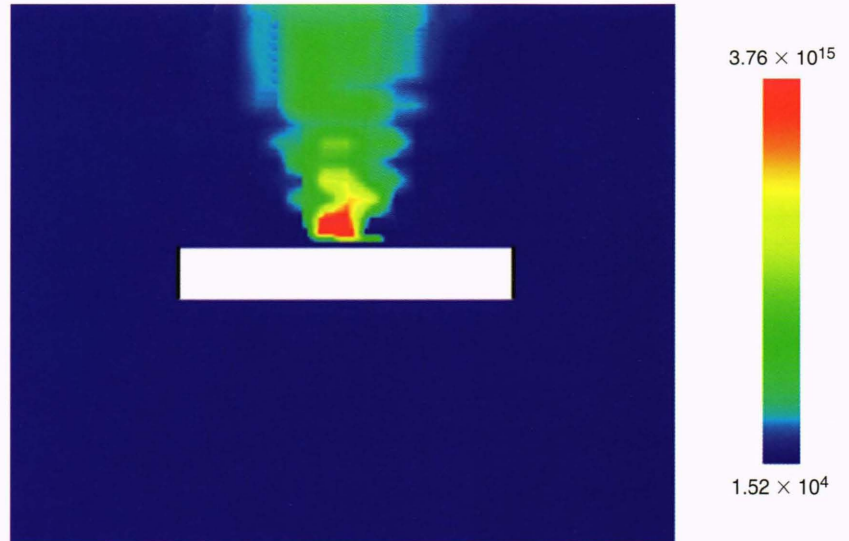


Figure 3. The density of argon (atoms/ m^3) issuing from a source slightly above a satellite traveling at approximately the same speed, altitude, and inclination as the one in Figure 2. The viewing point is from the side. The density scale is shown to the right of the figure.



defined velocity. Consider a frame of reference moving with the spacecraft (see Fig. 1) in which the ambient atmosphere, mostly oxygen atoms, is moving to the right with a constant velocity \mathbf{v}_a , and the flux of beam molecules is moving away from the source with a velocity \mathbf{v}_b . With only a single collision, beam molecules can only return along a ray inside the initial flux cone. This determines the return flux direction

$$\hat{\mathbf{v}}'_b = -\hat{\mathbf{v}}_b, \quad (3)$$

where $\hat{\mathbf{v}}_b$ is a unit vector in the direction of \mathbf{v}_b . So far this is simple kinematics. Conservation of momentum and energy then determines the magnitude of \mathbf{v}'_b .

In a quasi-steady state, the contribution to the return flux of molecules colliding with the ambient atmosphere in some volume element \mathbf{s}, ds and returning along the ray

$-\hat{\mathbf{v}}_b$ will be equal to the product of the magnitude of the initial flux in that direction (see Equations 1 and 2); the probability of the molecule reaching that point undeflected,⁷ $e^{-s/L}$; the scattering volume element, $s^2 ds d\bar{\Omega}$; the differential scattering cross section in the laboratory frame of reference, $I_{\text{lab}}[\bar{\chi} \equiv \cos^{-1}(\mathbf{v}_b \cdot \mathbf{v}'_b)]$; the number of scatterers, n_a ; the solid angle subtended by the spacecraft, $(4\pi s^2)^{-1} dA_{\text{sc}}$; and the probability of reaching the origin undeflected, $e^{-s/L}$:

$$\Delta j_{\text{ret}}(-\hat{\mathbf{v}}_b | s, ds) = n_b(R) v'_b n_a R^2 I_{\text{lab}}(\bar{\chi}) e^{-2s/L} (4\pi s^2)^{-1} d\bar{\Omega} dA_{\text{sc}} ds. \quad (4)$$

For very large mean free paths, the exponentials may be set equal to unity, and the total return flux along this ray is obtained by integrating from $s = R$ to $s \approx \infty$:

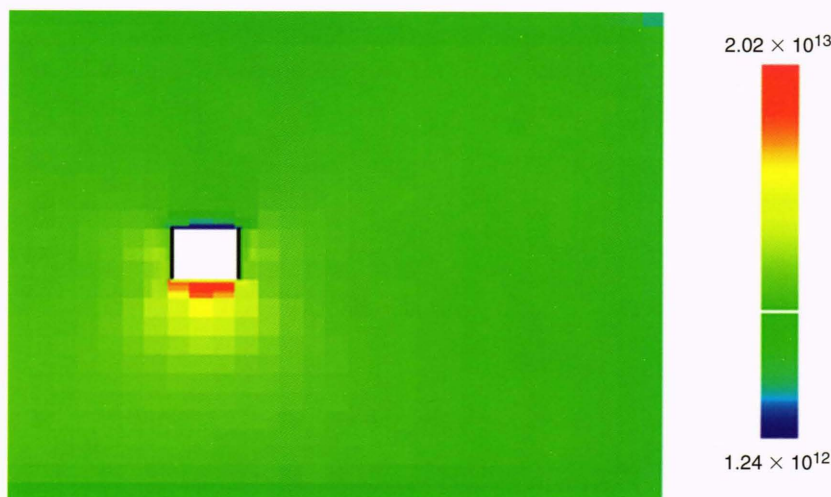


Figure 4. The density of oxygen (atoms/m³) in a plane perpendicular to the ram direction and amidships to a satellite traveling at approximately the same speed, altitude, and inclination as the one in Figure 2. The viewing point is from the front. The break in the density scale shown to the right of the figure corresponds to the undisturbed ambient oxygen atoms.

$$j_{\text{ret}}(-\hat{\mathbf{v}}_b) \approx n_b(R) v'_b n_a R e^{-2R/L} I_{\text{lab}}(\bar{\chi}) (4\pi)^{-1} d\bar{\Omega} dA_{\text{sc}}, \quad (5)$$

where we have used the relation

$$\int_x^\infty t^{-2} e^{-t} dt = x^{-1} e^{-x} + Ei(-x) \approx x^{-1} e^{-x} - \ln(\gamma x),$$

where $\ln \gamma \equiv 0.577215665$ (Euler–Mascheroni constant) and Ei denotes the exponential integral. As shown in a later section, Equation 5 may be made the basis of a back-of-the-envelope calculation of the return flux to a satellite orbiting at very high altitudes. To determine molecular potential energies, it is most convenient to work with the differential scattering cross section in the center of mass coordinate system, $I_{\text{cm}}(\chi)$, rather than $I_{\text{lab}}(\chi)$. The two scattering cross sections are related by the Jacobian for the transformation between the laboratory and center of mass coordinate systems. The explicit forms of the Jacobian and of the scattering angle χ will be given in the next section.

From the derivation, it is apparent that 99% of the return flux originates from distances $\leq 10R$; since the product of the ambient density and the differential scattering cross section is inversely proportional to the mean free path L , the total return flux from the first collision is on the order of R/L . With a little analytic geometry and the central limit theorem of probability, it can be shown that the return flux originating with all subsequent collisions with the ambient atmosphere will be on the order of R^2/L^2 .

COLLISION KINEMATICS AND CONSERVATION LAWS

In this section, the kinematics⁷ of the collision will be used to demonstrate that (1) the inclusion of single collision dynamics places strict limitations on the permissible return directions and (2) that within these limitations it is possible to deduce from experiment a center of mass

differential scattering cross section defined in an unusual cut in the three-dimensional volume generated by the energy/scattering angle/differential scattering cross section. It will then be argued that at the very high velocities that satellites orbit the Earth, these data can be used to determine molecular forces.

The center of mass velocity \mathbf{G} and relative collisional velocity \mathbf{g} are defined as follows:

$$\mathbf{G} \equiv M_a \mathbf{v}_a + M_b \mathbf{v}_b, \quad (6)$$

$$\mathbf{g} \equiv \mathbf{v}_b - \mathbf{v}_a, \quad (7)$$

where

$$M_i \equiv m_i / (m_a + m_b), \quad i = a, b. \quad (8)$$

The variables m_a and m_b refer to the masses of the ambient and beam molecules, respectively. Similar equations hold for the velocities after collision, i.e., \mathbf{G}' , \mathbf{g}' , \mathbf{v}'_a , \mathbf{v}'_b . So far this discussion has included only kinematics. Newton's laws impose certain global constraints on the possible values of the post-collision velocities. These constraints take the form of conservation laws. The first, conservation of momentum, requires that $\mathbf{G}' = \mathbf{G}$. For elastic collisions, conservation of energy requires that $|\mathbf{g}'| = |\mathbf{g}|$. Equations 6 and 7 may be inverted to yield

$$\mathbf{v}_b = \mathbf{G} + M_a \mathbf{g}, \quad (9)$$

$$\mathbf{v}'_b = \mathbf{G} + M_a \mathbf{g}'. \quad (10)$$

The combined effect of the two conservation laws can be shown graphically in what has become known as a "Newton diagram." The Newton diagram in Figure 5 shows that by construction, the heads of the vectors \mathbf{v}_b , $M_a \mathbf{g}$, and $M_a \mathbf{g}'$ must all lie on a circle that has a radius of magnitude $|M_a \mathbf{g}|$ and an origin coinciding with the head of \mathbf{G} . By construction, it is easy to see that a necessary

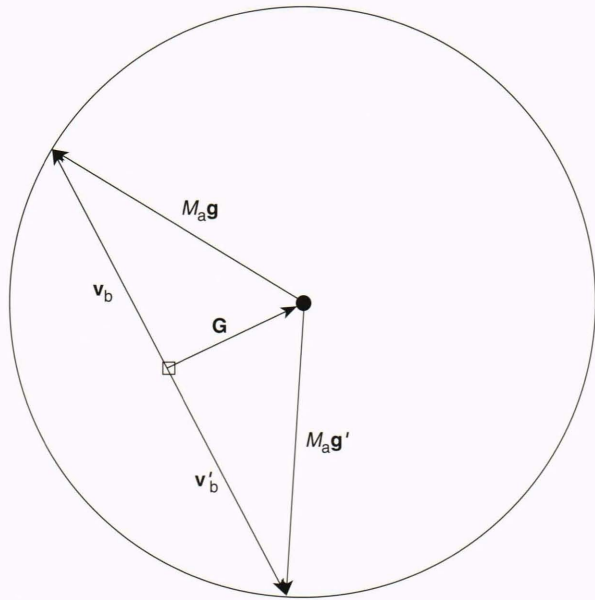


Figure 5. Newton diagram for elastic scattering. \mathbf{G} is the center of mass velocity, \mathbf{g} is the relative collisional velocity, M_a is the ratio of the mass of ambient atmospheric molecules to the sum of the masses of ambient and beam molecules, and \mathbf{v}_b and \mathbf{v}'_b are the prior and post collision velocities of the beam molecules, respectively.

condition for $\hat{\mathbf{v}}'_b$ to be equal to $-\hat{\mathbf{v}}_b$, i.e., Equation 3, is that

$$|\mathbf{G}| \leq |M_a \mathbf{g}|. \quad (11)$$

The angle $\bar{\theta}$ between the initial beam velocity and the initial ambient velocity is defined as

$$\bar{\theta} = \cos^{-1}(\hat{\mathbf{v}}_a \cdot \hat{\mathbf{v}}_b). \quad (12)$$

In terms of $\bar{\theta}$, Equation 11 becomes

$$\cos \bar{\theta} \leq \frac{(M_a - M_b) v_b}{2M_b v_a}. \quad (13)$$

For equal masses, this equation predicts that return fluxes exist for $0.5\pi \leq \bar{\theta} \leq \pi$. As the ratio of masses, M_b/M_a , increases, the lower limit of $\bar{\theta}$ approaches π , narrowing the range of angles in which return fluxes are possible with one elastic collision in the ambient atmosphere. The critical value of the mass ratio below which return fluxes are possible is determined by Equation 11, which for $\bar{\theta} = \pi$ becomes

$$\mathbf{v}'_b = 2M_a \mathbf{v}_a + (M_a - M_b) \mathbf{v}_b = 0. \quad (14)$$

A related angle of interest is the angle θ defined by

$$\theta \equiv \cos^{-1}(\hat{\mathbf{v}}_b \cdot \hat{\mathbf{g}}) = \pi - \cos^{-1}(\hat{\mathbf{v}}'_b \cdot \hat{\mathbf{g}}). \quad (15)$$

An angle of more direct physical interest, as we shall see later, is the scattering angle in the center of mass frame of reference:⁷

$$\chi \equiv \cos^{-1}(\hat{\mathbf{g}} \cdot \hat{\mathbf{g}}'). \quad (16)$$

Treating v_b , g , and θ as knowns, Equations 9, 10, 15, and 16 may be solved to yield relations for v'_b and χ :

$$g^{-2} \left\{ M_a^{-2} (v'_b - v_b)^2 \sin^2 \theta + \left[g - M_a^{-1} (v'_b + v_b) \cos \theta \right]^2 \right\} = 1, \quad (17)$$

$$\chi = \cos^{-1} \left[1 - \frac{1}{g M_a} (v'_b + v_b) \cos \theta \right]. \quad (18)$$

The differential scattering cross section in the laboratory coordinate system is just the product of the differential scattering cross section in the center of mass coordinate system and the Jacobian⁸ for transformation between the two coordinate systems, $d\omega_{\text{cm}}/d\bar{\Omega}$. By the Liouville theorem, the latter is the product of the ratio of the areas subtended by \mathbf{v}'_b and $M_a \mathbf{g}'$ and the angle between the normals to the two areas:

$$d\omega_{\text{cm}}/d\bar{\Omega} = (v'_b/M_a g')^2 / |\hat{\mathbf{v}}'_b \cdot \hat{\mathbf{g}}'|, \quad (19)$$

so that

$$v_b I_{\text{lab}}(\bar{\chi}) = g I_{\text{cm}}(\chi) [(v'_b/M_a g')^2 / |\hat{\mathbf{v}}'_b \cdot \hat{\mathbf{g}}'|]. \quad (20)$$

In conjunction with Equations 17, 18, and 20, Equation 5 may now be used to infer $I_{\text{cm}}(\chi)$ from experimental return fluxes, and, with the analysis of the next section, molecular forces.

COLLISION DYNAMICS

The scattering angle χ is a function of (1) the kinetic energy E of relative motion in the center of mass frame,^{7,8} (2) the component of force, $\mathbf{F}_r = \hat{\mathbf{r}} \partial V / \partial r$ (where V is the potential energy), in the direction, $\hat{\mathbf{r}}$, connecting the centers of mass of the two colliding molecules, and (3) the angular momentum of the collision, \mathbf{M} . Since \mathbf{F}_r as written is a conservative force field, the collision is confined to a plane; \mathbf{M} is a vector oriented perpendicular to the plane, and its magnitude and orientation are constants of motion. In the conservation of momentum relation,

$$M_y = \mu (g_y x - g_x y) \underset{r \rightarrow \infty}{\approx} \mu g b, \quad (21)$$

where

$$\mu \equiv m_a m_b / (m_a + m_b), \quad (22)$$

b is the distance of closest approach that would have been achieved if the force, which deflects the relative motion from a straight line, had not been present. The differential scattering cross section, well known as the probability of being scattered into a solid angle $\sin \chi d\chi d\varphi$, is⁸

As a second approximation, we assume that orbital velocities are much greater than beam velocities so that we can set $M_{ag} \gg v_b$. This approximation leads to $g \approx v_a$ and $\bar{\theta} \approx \theta$. Equation 17 may now be replaced by

$$v'_b \approx 2M_a v_a \cos \bar{\theta}. \quad (31)$$

With this simplification, the return flux now assumes a very simple approximation that can truly serve as a back-of-the-envelope approximation:

$$\begin{aligned} j_{\text{ret}}(-\hat{v}_b) &\approx n_b(R) \frac{R}{4\pi^2 L} e^{-2R/L} v_a |\cos \bar{\theta}| d\bar{\Omega} dA_{\text{sc}}, \\ &\cos^{-1} \frac{(M_b - M_a)v_b}{2M_a v_a} \leq \bar{\theta} \leq \pi, \\ &= 0, \quad \text{otherwise.} \end{aligned} \quad (32)$$

The limitations come from Equation 11. This simple form predicts that at high altitudes, the return flux is proportional to the beam and ambient densities, the spacecraft velocity, and the spacecraft radius; it is inversely proportional to the mean free path, and it is strongly peaked in the forward direction, that is, when the effluent flux is exactly in the ram direction.

DISCUSSION

The high peaking toward the ram direction comes not only from the explicit appearance of $\cos \bar{\theta}$ in Equation 32, but also from the limitations resulting from the inequality of Equation 11. This means that as the mass of the beam molecule increases, the window of angles within which observations can be made decreases and finally vanishes for some finite mass ratio. The resolution consequently also deteriorates. Another limitation arises because returning molecules start the return legs of their trajectories at all points along the ray. Thus, the pulsed beam source suggested in the previous section would show its peak sensitivity at short times. To see this, note that the asymptotic variation of the return flux signal at long times would be approximately t^{-2} for both elastically and inelastically scattered molecules. A velocity analyzer would then be needed to distinguish between the two types of collision. Against these disadvantages, one can cite the almost uniform speed and distribution of oxygen atoms flowing past the spacecraft.

Some limitations in the experiment or in the analysis could be lifted. Pulsing the source would increase the signal-to-noise ratio and provide a means, in principle, of resolving elastic and inelastic collisions. Providing the detector with a set of skimmers or a quadrupole analyzer might define the direction of the return flux sufficiently to run the experiment at lower altitudes where one cannot approximate the spacecraft by a point. With a narrow source beam and quadrupole analyzer, however, all the preceding analysis could be applied to this case with one substantial change: the allowance for a small distance-dependent deviation of the direction of the return beam from the source beam direction. Exciting the beam molecules would generate information on superelastic scattering. Finally, the eikonal approximation could be lifted and replaced by the exact expression⁸ for the scat-

tering angle, χ , but doing so would complicate the analysis considerably. An easier method might be the following: The eikonal approximation (Equation 25) is not quite correct because it predicts a scattering angle that approaches infinity as b approaches 0 rather than π , which is the $b \rightarrow 0$ asymptote of the more correct semi-classical scattering angle:¹³

$$\chi = \pi - \int_{r_{\text{min}}}^{\infty} r^{-2} \left[b^{-2} \left(1 - \frac{V}{E} \right) - r^{-2} \right]^{-1/2} dr. \quad (33)$$

The term r_{min} , the classical distance of closest approach, is given by the minimum finite distance where the term in brackets in Equation 33 vanishes. Nevertheless, the eikonal approximation is useful as an approximation at moderate to large values of b to estimate the potential at moderate to large distances. We note that at small values of b , which correspond to more or less head-on collisions, the collision energy is relatively insensitive to $\bar{\theta}$ and can be approximated by E_{max} , the maximum collision energy. In Equation 33, at large to moderate values of r , $V(r)$ can be approximated by the eikonal estimate, $V_{\text{eik}}(r)$, which can be determined by the inversion carried out in Equation 26, and χ can be determined at moderate values of b . These estimates of χ at moderate to large values of b can now be paired into the observed $\chi[b, E(v_b)]$ at smaller b . The new constant-energy scattering angle, $\chi[b, E(v_{\text{max}})]$, can now be put into the form of an Euler transform,¹³ which can also be inverted by the standard methods of inverting Abel integral equations.^{13,14} The appearance of these two names, Abel and Euler, once again indicates that good science, in this case good mathematics, is, in a sense, timeless and will always have its uses. Here, it plays a central part in the interpretation of the proposed experiment. For the experiment itself, all one needs is a satellite at high altitude, a well-defined molecular beam, and a good detector.

REFERENCES

- Rios, E. R., and Rodriguez, R. T., *MOLFLUX: Molecular Flux User's Manual*, NASA (Feb 1989).
- Robertson, S. J., "Bhatnagar-Gross-Krook Model Solution of Back-Scattering of Outgas Flow from Spherical Spacecraft," *Prog. Astronaut. Aeronaut.* **51**, 479-489 (1977).
- Robertson, S. J., *Spacecraft Self-Contamination due to Back-Scattering of Outgas Products*, Report No. LMSC-IIREC-TR-196676, Lockheed Research and Engineering Center (Jan 1976).
- Tran Cong, T., and Bird, G. A., "One-Dimensional Outgassing Problem," *Phys. Fluids* **21**, 327-333 (1978).
- Bird, G. A., "Spacecraft Outgas Ambient Flow Interaction," *J. Spacecr.* **18**, 31-35 (1981).
- Hueser, J. E., Melfi, L. T., Jr., Bird, G. A., and Brock, F. J., "Rocket Nozzle Lip Flow by Direct Simulation Monte Carlo Method," *J. Spacecr.* **23**, 363-367 (1986).
- Chapman, S., and Cowling, T. G., Chap. 3 in *The Mathematical Theory of Non-Uniform Gases*, Cambridge University Press (1970).
- Levine, R. D., and Bernstein, R. B., *Molecular Reaction Dynamics and Chemical Reactivity*, Oxford University Press, pp. 91-94 (1987).
- Brackett, J. W., Mueller, C. R., and Sanders, W. A., "Direct Determination of Scattering Phase Shifts from Differential Cross Sections," *J. Chem. Phys.* **39**, 2564-2571 (1963).
- Vollmer, G., "Inverse Problem in Atom-Atom Scattering in WKB Approach," *Z. Physik* **226**, 423-424 (1969).
- Klingbeil, R., "Determination of Interatomic Potentials by the Inversion of Elastic Differential Cross Section Data. I. An Inversion Procedure," *J. Chem. Phys.* **56**, 132-136 (1972).
- Remler, E. A., "Complex-Angular-Momentum Analysis of Atom-Atom Scattering Experiments," *Phys. Rev. A* **3**, 1949-1954 (1971).

- ¹³Newton, R. C., *Scattering Theory of Waves and Particles*, Second Edition, Springer-Verlag, New York, pp. 600-605 (1982).
- ¹⁴Whittaker, E. T., and Watson, G. N., *Modern Analysis*, Cambridge University Press, Section 11.8 (1950).
- ¹⁵Monchick, L., "A Comment on the Inversion of Gas Transport Properties," *J. Chem. Phys.* **73**, 2929-2931 (1980).

THE AUTHOR



LOUIS MONCHICK was born in New York, raised in Boston, and educated at Boston University, where he received his Ph.D. in 1954. He held a post-doctoral fellowship at the University of Notre Dame from 1954 to 1956. He came to APL in 1957, where he has remained except for short visits to the JHU Homewood campus as part-time assistant professor and as Parson's Professor, and to the universities of Bielefeld and Leiden as a visiting scientist. Dr. Monchick has worked in the fields of diffusion-controlled reactions, molecular collision phe-

nomena, transport properties of polyatomic molecules, and line shapes of Raman scattering spectra. Two of his publications made the "twenty-two most cited" list of articles published by APL staff members [Berl, W. G., *Johns Hopkins APL Tech. Dig.* **7**(3), 221 (1986)]. He was also the guest editor of a recent issue of the *Digest* (Vol. 12, No. 3, 1991).